Stepwise investigation of the influences of steric groups versus counter ions to target Cu/Dy complexes

Irina A. Kühne,[a,b†] Kieran Griffiths,[b] Amy-Jayne Hutchings,[a] Oliver P. E. Townrow,[b] Andreas Eichhöfer,[c] Christopher E. Anson[a] George E. Kostakis,*[,b] and Annie K. Powell*[,a,c]

[a] Institut für Anorganische Chemie, Karlsruher Institut für Technologie, Engesserstrasse 15, 76131 Karlsruhe, Germany;

[b] Department of Chemistry, School of Life Sciences, University of Sussex, Brighton BN1 9QJ, United Kingdom;

[c] Institut für Nanotechnologie, Karlsruher Institut für Technologie, Hermann-von-Helmholtz-Platz 1, 76344 Eggenstein-Leopoldshafen, Germany.

ABSTRACT: From an investigation of varying the steric bulk of a flexible ligand, we have produced a family of structures using similar reaction conditions. Even small changes from a hydrogen atom to a methyl to an ethyl group on the ligand influences the structural outcome, which can also be steered by the nature of the metal source. We employed Schiff base ligands by combining *o*-vanillin and three different 2-amino-1,3-propandiol units, leading to H_3L_1 (R=hydrogen), H_3L_2 (R=methyl) and H_3L_3 (R=ethyl). The differing nuclearities of the three clusters, **1** to **3**, originate mainly from the steric influence, while this effect is not seen in complex **4** to **6**, where the general butterfly motif is maintained. We present here the synthesis, crystal structures and magnetic properties of six new Cu^{II}-Ln^{III} complexes, providing valuable insight into future synthetic directions. The topological part includes a table of all Cu^{II}-Dy^{III} complexes with nuclearities higher than four and their topological motif. The investigation of the magnetic behaviors reveal that all six complexes show frequency dependent signals in the out-of phase ac susceptibility, which is indicative for SMM behavior.

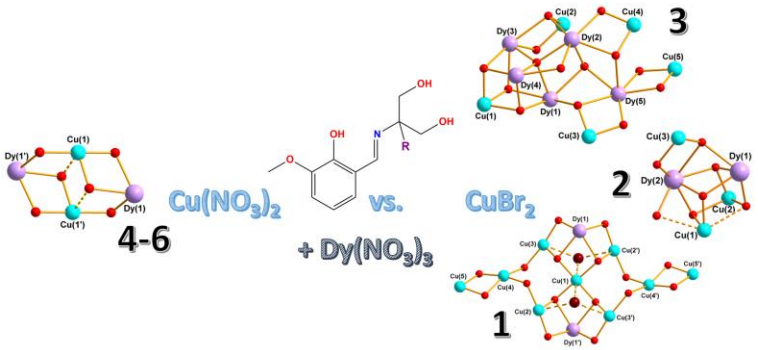

Introduction

Since the discovery of Single Molecule Magnets (SMMs) exemplified by mixed valence polynuclear Mn12 carboxylate coordination clusters in the early 90s,[1,2] such coordination clusters have attracted much attention, not only due to their possible applications,[3,4] but also due to the investigation of the fundamental aspects of magnetic interactions and magneto-structural correlations.[5–7] These are necessary in order to design new molecular-based magnets. Polynuclear complexes based on transition metals and/or lanthanide ions were studied as SMMs[6,8–11] and, more recently, interest in mixing 3d and 4f ions within coordination complex based systems such as 1-D chains and zero dimensional coordination clusters have been widely studied.[6,7] However, amongst these, Cu^{II}-Ln^{III} systems have received relatively little attention in terms of their SMM properties up to now.[12–20] Nevertheless, it is advantageous for complexes to combine highly anisotropic 4f ions such as Dy^{III} with the quantum spin Cu^{II} d^9 ion. In the case of Cu^{II}-Dy^{III} dimers, which are incorporated into the pockets available in Schiff base ligands incorporating *o*-vanillin, the coupling between these metal centers is often observed to be ferromagnetic.[21,22] This can even be seen in bigger clusters, where ferromagnetic behavior is still dominant, leading to enhancement of the magnetic behavior, as seen, for example, in Cu_8Dy_3,[23] Cu_6Gd_6,[24] Cu_6Ln_2,[25] Cu_5Ln_2 [26] and Cu_4Dy_4.[27]

We previously showed that by replacing the alcohol group of the "tris" ligand, where tris = tris-(hydroxy-methyl)aminoethane, with an ethyl group, leading to the ligand H_3L_3, 2-ethyl-2-((2-hydroxy-3-methoxybenzyl-idene) amino)propane-1,3-diol and see Scheme 1, it is possible to adapt the synthesis of Cu_5Ln_2 compound[28] to produce a related, but expanded, Cu_9Ln_2 compound.[29] Here we describe our effort to test the boundaries of this system by "fine-tuning" the ligand to test its limits. Thus, we explored the further effects of changing the ethyl group to a methyl group in addition to completely exterminating alkyl group steric influence. These endeavors have led to new crystal structures containing a plethora of molecules with interesting topologies and varied magnetic properties.

The motivation for this is the fact that it is currently almost impossible to predict the outcome of the synthesis of 3d-4f clusters in terms of their nuclearities and overall core structures. This is particularly so when the 3d partner has a plastic coordination geometry, usually dictated by the relative importance of crystal/ligand field effects which can be counted as the first order perturbation for these ions. Particularly susceptible to these effects are ions such as Cu^{II} as a Jahn-Teller d^9 system and the Fe^{III} high spin d^5 system. In the latter case, the lack of any ligand field stabilization energy leads to manifold distortions of the local coordination geometry of the 3d ion and therefore more possibilities for accessing excited states, whilst in the former case, the need to lift the degeneracy of the unequally occupied e_g orbitals in octahedral ligand fields leads to a wide variety of 4, 5 and 6 fold coordination geometries.[30,31]

Nevertheless, such ions (both of which can be counted as quantum spins at the purest level) when combined with 4f metal ions can produce some of the most intriguing 3d-4f single molecule magnets.[32–35] A key factor seems to be the nature of both the 3d coordination geometry and that of the 4f ion. When looking at the impressive, very large Cu^{II}-Dy^{III} clusters found in the literature,[19,20,27,29,36–51] it is clear that it is difficult to understand the formation pathways and to analyze the details of the individual coordination sphere of the 3d and 4f ions. On the other hand, a systematic investigation of smaller 3d-4f clusters, and in particular, as we report here, for Cu^{II}-Dy^{III} clusters which result from small stepwise changes in the synthetic route and where the ligand differs only in the non-coordinating part, gives insights into the directing properties of the ligand and thus for further ligand design.

Here we report the synthesis and characterization of six new Cu^{II}-Dy^{III} clusters and incorporate their topological description into a Cu^{II}-Dy^{III} topological database.

Results and Discussion

Synthetic Strategy. The syntheses of the different ligands and reaction conditions for each compound can be found in the experimental section. We choose Schiff base ligands derived from *o*-vanillin since these have two pockets which can capture metal ions, in some case these can be ions with differing HSAB character and differing coordination requirements.[52] Here one pocket is formed by the phenoxo oxygen and the imine nitrogen, labelled as pocket 1 from now on. The second pocket, which is defined by the phenoxo and the methoxy oxygens, can incorporate either one Cu^{II} or one Dy^{III} ion but can also remain vacant, and is from now on labelled as pocket 2, see Scheme 1.

Scheme 1. Available pockets derived from *o*-vanillin for metal coordination within ligands H_3L_1 to H_3L_3, with R = hydrogen (L_1), methyl (L_2) and ethyl (L_3).

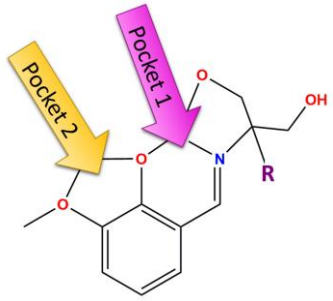

We followed a synthetic route where we scanned all combinations of either $Cu(NO_3)_2{\cdot}3H_2O$ or $CuBr_2$ along with $Dy(NO_3)_3{\cdot}6H_2O$ and the related Schiff base ligands with R = ethyl (L_3), methyl (L_2) or hydrogen (L_1), see Scheme 2 and Table 1. Using the previously reported synthetic method for complex **1**, $[Cu_9Dy_2(\mu_3\text{-}OH)_4(\mu_3\text{-}Br)_2(L_3)_2(HL_3)_4(Br)_2(NO_3)_2(MeOH)_4]$,[29] we observed that the combinations containing bromide ions lead to three completely different structures with the three ligands (**1** to **3**). On the other hand, we can see a clear trend when nitrate counter ions are available. In this case, it seems that the differences in steric influence of the different ligands has no impact on the structure and a butterfly Cu_2Dy_2 compound (**4** to **6**) is always isolated. Complex **1**, a Cu_9Dy_2 compound, was previously published,[29] but was the origin of this endeavor, and therefore will be mentioned in some parts of the following analysis.

Scheme 2. Ligands H_3L_1, H_3L_2 and H_3L_3.

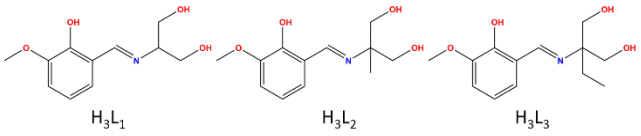

Table 1. Reaction conditions leading to the formation of complex **1** to **6**.

$Dy(NO_3)_3$ +	H_3L_3	H_3L_2	H_3L_1
$CuBr_2$	Cu_9Dy_2 (**1**)[29]	Cu_3Dy_2 (**2**)	Cu_5Dy_5 (**3**)
$Cu(NO_3)_2$	Cu_2Dy_2 (**4**)	Cu_2Dy_2 (**5**)	Cu_2Dy_2 (**6**)

Structural Description.

Complex **1**, $[Cu_9Dy_2(\mu_3\text{-}OH)_4(\mu_3\text{-}Br)_2(L_3)_2(HL_3)_4(Br)_2(NO_3)_2(MeOH)_4]$ will not be described here, but is mentioned for completeness of the analysis. For the structural description see Powell et al.[29]

Under similar synthetic conditions as used to obtain complex **1**, but replacing the ethyl group on the ligand

(H_3L_3) with a methyl group (H_3L_2) (see Scheme 2), we were able to crystallize a pentanuclear compound. Complex **2**, $[Cu_3Dy_2(\mu_3\text{-}OH)(L_2)(HL_2)_3(H_2L_2)(MeOH)_2]Br\cdot 4MeOH$ crystallizes in the monoclinic space group $P2_1/c$ with Z = 4. The structure of **2** is shown in Figure 1, together with its core structure, which helps to illustrate the connection modes between the different metal centers. The core has some similarities to a previously published Cu_3Ln_2 structure from Vaz et al. [53]

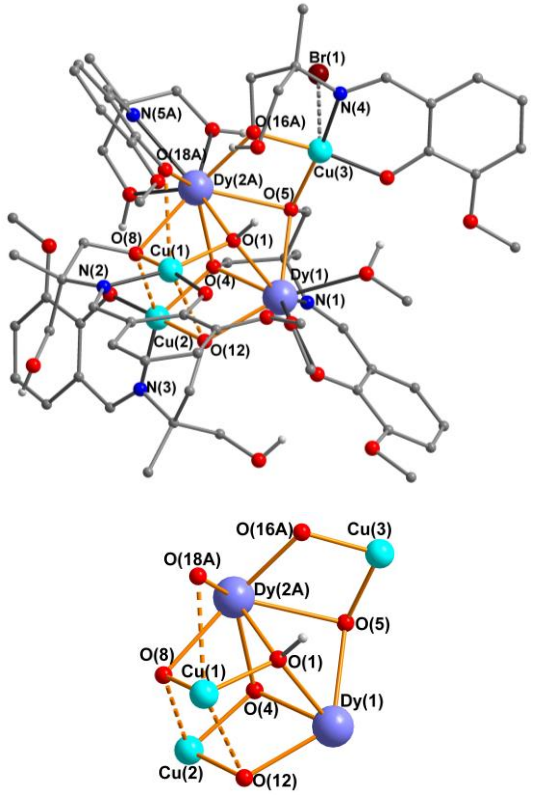

Figure 1. Molecular structure of Cu_3Dy_2 (**2**) (above) and its cluster core (below). Organic H atoms and minor disorder omitted for clarity, bridging Cu-O and Dy-O highlighted in orange, Cu^{II} Jahn-Teller axes shown as dashed lines.

Interestingly, there are five L_2 ligands chelating the five metal centers in complex **2**, with three different coordination modes, see Scheme 3. Three out of five ligands are doubly-deprotonated, HL_2, (Scheme 3, left).

Scheme 3. Different coordination modes of L_2 in Cu_3Dy_2 (**2**).

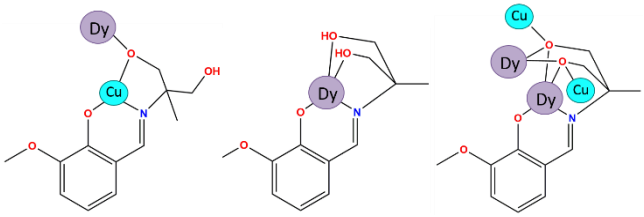

All three each chelate one Cu^{II} ion in pocket 1. The chelating diol oxygen additionally links to a Dy^{III} ion. The one singly-deprotonated ligand, H_2L_2, chelates to Dy(2), (Scheme 3, middle) which is incorporated into pocket 1. The fully deprotonated ligand, L_2, (Scheme 3, right) shows an unusual but very symmetric coordination mode and builds the link between four metal centers, due to the fact that both diol arms of the ligand, O(4) and O(5) are each μ_3-bridging between both Dy^{III} ions and one Cu^{II}. This leaves a single copper ion Cu(1) not coordinated by this ligand.

Compound **3**, $[Cu_5Dy_5(\mu_4\text{-}O)(\mu_3\text{-}OH)_3(L_1)_3(HL_1)_4(NO_3)_2(MeOH)_2]$ $[Cu_5Dy_5(\mu_4\text{-}O)(\mu_3\text{-}OH)_3(L_1)_3(HL_1)_4(NO_3)(MeOH)_3(H_2O)](NO_3)\cdot H_2O\cdot 25MeOH$ crystallizes in the triclinic space group $P\bar{1}$ with Z = 2. In the asymmetric unit there are two crystallographically-independent but almost isostructural Cu_5Dy_5 coordination clusters, which differ only in the peripheral ligands chelating Dy(3) and Dy(4) in molecule 1, and the corresponding atoms Dy(8) and Dy(9) in molecule 2. Detailed crystallographic parameters are given in Table S1.

The complete structure of cluster molecule 1 in compound **3** is shown in Figure 2, together with the central core, in which the central Dy_5 polyhedron is highlighted. The structure consists of a tetrahedron of Dy^{III} ions, Dy(1) to Dy(4), around a μ_4-oxygen, O(1), with the four Dy-O(1) bonds shown as pink in Figure 2. One edge of this Dy4 tetrahedron, Dy(1)-Dy(2), is then shared with a Dy3 triangle defined by Dy(1), Dy(2) and Dy(5).

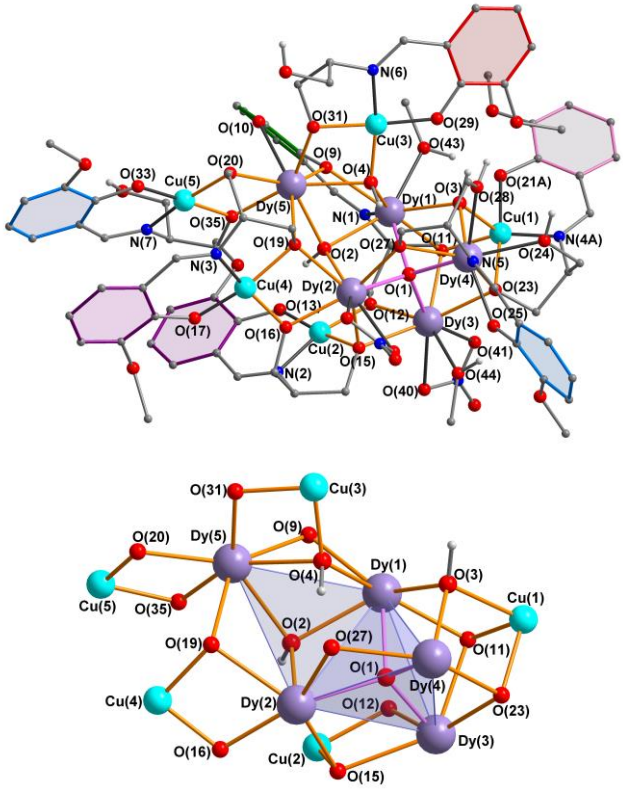

Figure 2. Molecular structure of Cu_5Dy_5 cluster 1 in **3** (above) and its cluster core (below). Organic H atoms omitted for clarity, Dy-(μ_4-O) bonds pink, remaining bridging Cu-O and Dy-O bonds orange; aromatic rings highlighted according to coordination mode of their respective ligand, see Scheme 4), Dy5 polyhedron in the core highlighted for clarity.

At the same time, a slightly distorted heterocubane is built up by Cu(1) together with Dy(1), Dy(3) and Dy(4), three μ_3-oxygens, O(3), O(11) and O(23), and the μ_4-oxygen, O(1). Cu(2), Cu(3) and Cu(4) are each linked by a μ_3-bridge and an additional μ_2-bridge to two neighboring Dy^{III} ions. Cu(5) is only linked by two μ_2-bridges to Dy(5) and is therefore a dangling rather than a bridging entity in relation to the Dy_5 core.

In total, there are seven L_1 Schiff base ligands in the structure, labelled according to their nitrogen atom. Within the structure these seven Schiff base ligands show five different coordination modes, which are summarized in Scheme 4 and are highlighted in different colors to help locating them within the complex shown in Figure 2. Ligands 1 to 3 are fully deprotonated, while ligands 4 to 7 are only doubly deprotonated with one diol oxygen still protonated. Ligands 2 and 3 show the same coordination mode, as do ligands 6 and 7. The great coordinative flexibility of the ligand makes it possible to connect up to five metal ions. Thus, although complexes **1** and **2** have already shown a great variety of coordination modes concerning their ligands, here the variety is even greater. As seen in the previous two complexes, pocket 2, which is more flexible in incorporating metal ions, is in this complex only occupied for ligand 1 with a Dy^{III} ion, otherwise remains vacant. Pocket 1 instead, is either occupied by a Cu^{II} or a Dy^{III} ion, which is then additionally chelated by one of the diol oxygens. Only in the case of ligand 5 do both diol oxygens chelate the Dy^{III} ion which is incorporated into pocket 1.

Scheme 4. Coordination modes of the organic ligands in Cu_5Dy_5 (**5**), (ligands numbered according to their N atom; ligands 2 and 3 have the same coordination mode, as do ligands 6 and 7).

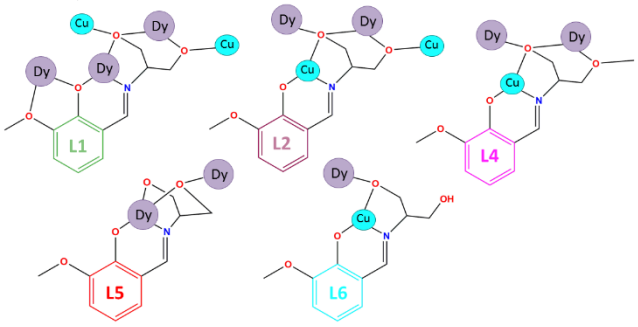

In order to investigate the origin of the structural differences between these three complexes, it is helpful to show the coordination modes of ligand L_3 within the previously reported Cu_9Dy_2 (**1**) here as well (see Scheme 5).[29] There are several rationales on comparing the different coordination modes leading to the three different structures.

First of all, the steric impact of the ethyl group in ligand H_3L_3 has to have an effect on the ligand coordination, especially on the flexibility of the diol arms. In the case of complex **3** we also have the special case of ligand 5 (see Scheme 4), where both diol oxygens chelate the Dy^{III} ion, which is incorporated into pocket 1. Obviously, this coordination mode was not observed in complex **1**. Instead we can see a similar coordination mode in the case of complex **2** (see Scheme 3). Thus, it seems that the methyl group does not have a strong steric influence, probably due to its smaller size.

Scheme 5. Coordination modes of H_3L_3 in Cu_9Dy_2 (**1**) (highlighted in colors related to Figure 1).

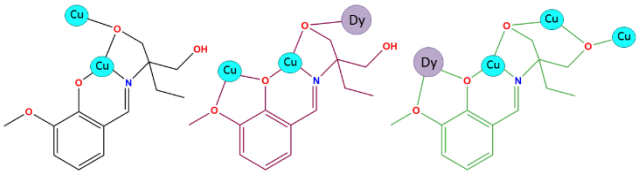

In a second attempt to figure out the origin of the differences in the complex formation, we had a closer look at the angles between the imine nitrogen atom, the sp^3 carbon atom next to it, and both of its neighboring carbon atoms (see Scheme 6 and ESI, Table S2). The average (N-C9-C10/11) bond angle increases from 105.95° for **1**, 106.66° for **2** and 108.45° for **3**. A similar trend was found for the angle which incorporates the sp^3 carbon atom C9 (C10-C9-C11), where the angles become more obtuse from 109.61° for **1**, to 111.05° for **2** and to113.29° for **3**. Both trends support the role of the steric impact of the ethyl group, which makes the ligand more rigid and thus the angles stay smaller in the case of complex **1**.

Scheme 6. Numbering of atoms within the Schiff base ligand with R = H (H_3L_1), Me (H_3L_2) and Et (H_3L_3).

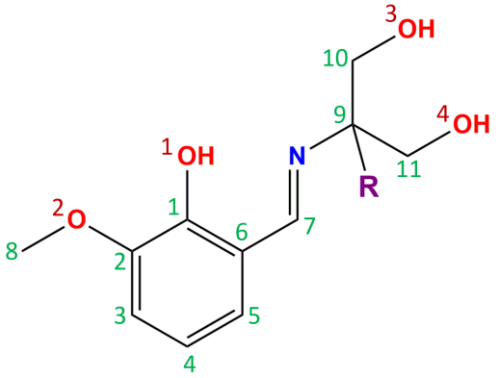

When using a metal ion mixture with only nitrate containing metal salts, under similar conditions as for complex **1** to **3**, isostructural butterfly Cu_2Dy_2 compounds (**4**, **5** or **6**) were obtained with all three ligands. $[Cu_2Dy_2(\mu_3\text{-}OMe)_2(HL_3)_2(NO_3)_4]\cdot 2MeOH$ (**4**) crystallizes in monoclinic $P2_1/n$ with Z = 2, and is isomorphous to compound **5**, $[Cu_2Dy_2(\mu_3\text{-}OMe)_2(HL_2)_2(NO_3)_4]\cdot 2MeOH$. $[Cu_2Dy_2(\mu_3\text{-}OMe)_2(HL_1)_2(NO_3)_4]$ (**6**) crystallizes differently, without lattice solvent, in monoclinic $P2_1/c$ with Z = 2, but the Cu_2Dy_2 cluster is still closely isostructural to those in **4** and **5**; all three clusters have crystallographic inversion symmetry. Detailed crystallographic parameters for all three complexes are given in Table S5. Therefore, complex **4**

will be described as typical for complexes **4** to **6**, shown in Figure 3.

The centrosymmetric butterfly structure of **4** has the "body" formed by two Cu^{II} ions and the "wings" by two Dy^{III} ions, with all four metal centers coplanar. Cu(1), Cu(1') and Dy(1) are bridged by the oxygen O(1) of a μ_3-OMe ligand, although this bridge is unsymmetrical, as Cu(1)-O(1) involves an equatorial site on Cu(1), whereas Cu(1')-O(1) defines the elongated Jahn-Teller axis of the Cu^{II} ion. Additionally, Cu(1) is bridged by two deprotonated μ_2-oxygens from the organic ligand to Dy(1) via O(2) and to Dy(1') via O(4). The Schiff base ligands in the structure are thus doubly-deprotonated, with the remaining alcohol arm coordinating to Dy(1'). Their bridging mode, see Figure 4 (right), is similar, but not the same, to the μ_3-bridging mode (purple in Scheme 5) observed in complex **1**.

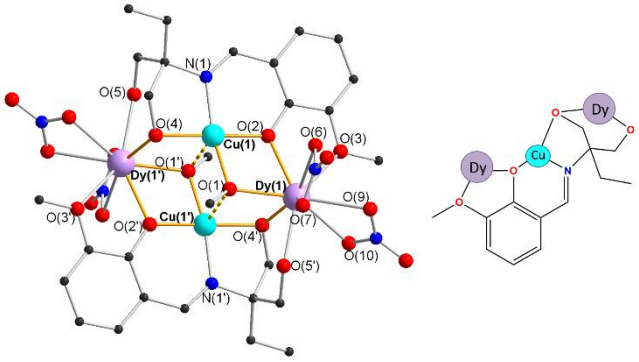

Figure 3. Molecular structure of Cu_2Dy_2 (**4**) (Hydrogen atoms omitted for clarity, all bridging Cu-O and Dy.O bonds orange) (left), and the coordination mode of HL_3 in Cu_2Dy_2 (**4**) (right).

Topological Analysis.

For the topological analysis we used the TOPOS software[54] which adopts the *N*D*k*-m[55] symbolism. This is a helpful method to describe coordination clusters that uses only monoatomic bridges to create a "decorated core" which in turn can be used to assess their similarities with clusters reported in the literature.

To date, the synthesis of polynuclear Cu/Dy CCs has received considerable attention and fifty-five compounds with nuclearities ranging from 4 to 60 have been previously reported (Table 2), with the ligands shown in Scheme S2, see ESI. Table 2 shows the abbreviated molecular formula, but the complete table can be found in the ESI, Table S3. The topological representation of these compounds is shown in Figure 4 and the organic ligands utilized for their synthesis are shown in Scheme S2, see ESI. Mostly Schiff base ligands have been used. The coordination pockets of the organic ligands used for the synthesis of the present Cu/Dy coordination complexes are similar; with the only variable being the R group and the anion (Br or NO_3). The ligands used in this study offer two pockets for coordination and the hydroxyl groups pose ideal candidates to bridge several metal centers.[56]

The topological representation of compounds **1** to **6** are shown in Figure 5. An automatic subgraph search, to correlate the lower nuclearity topologies (**4** to **6**) with the higher nuclearities (**1** to **3**), reveals that that the decorated motif of the three tetranuclear (**4** to **6**) and one pentanuclear compound, complex **2**, could not be identified, via the automatic graph procedure, within the decorated motif of the decanuclear complex **3** and undecanuclear compound **1**. The minor change on the organic backbone of the ligands L_1, L_2 and L_3, used in this study, leads to significant topological variations by using different Cu salts. The present work can be utilized as a database of polynuclear Cu/Dy CCs and analogous studies have been reported for Co/Ln and 3d/4f CCs.[57,58]

Table 2. Polynuclear Cu/Ln compounds with nuclearities equal to and higher than 4 and their structural motif detected with TOPOS.

Entry	Formula	Ligand	Nuclearity	Motif	Ref.
1	$Cu^{II}_2Dy^{III}_2$	**L25, HL26**	4	**1,2M4-1**	59
2	$Cu^{II}_2Dy^{III}_2$	H**L27**	4	**2,3M4-1**	60
3	$Cu^{II}_2Dy^{III}_2$	H**L28**, H**L29**	4	**2M4-1**	61
4	$Cu^{II}_2Dy^{III}_2$	**L30**	4	**1,2M4-1**	62
5	$Cu^{II}_2Dy^{III}_2$	H_3**L31**, H**L9**	4	**2M4-1**	63
6	$Cu^{II}_2Dy^{III}_2$	H**L33**	4	**2,3M4-1**	64
7	$Cu^{II}_2Dy^{III}_2$	H_3**L35**	4	**(1M2-1)2**	65
8	$Cu^{II}_2Dy^{III}_2$	H**L36**,**L37**	4	**1,2M4-1**	66
9	$Cu^{II}_2Dy^{III}_2$	H_2**L38**	4	**1,2M4-1**	67
10	$Cu^{II}_3Dy^{III}$	H_2**L40**	4	**1,2M4-1**	68
11	$Cu^{II}_3Dy^{III}$	H_6**L32**	4	**1,3M4-1**	69
12	$Cu^{II}_2Dy^{III}_2$	H_2**L42**	4	**4(0)**	70
13	$Cu^{II}_2Dy^{III}_2$	H**L41**	4	**2,3M4-1**	71
14	$Cu^{II}_3Dy^{III}$	H_4**L34**	4	**1,3M4-1**	72
15	$Cu^{II}_2Dy^{III}_2$	H_2**L43**	4	**(1)+(0)M4-1**	73
16	$Cu^{II}_2Dy^{III}_2$	**L55**	4	**4(0)**	74
17	$Cu^{II}Dy^{III}_4$	L1 , H_2**L2**	5	**2,4M5-1**	60
18	$Cu^{II}_4Dy^{III}$	H_2**L45**	5	**2,4M5-1**	20
19	$Cu^{II}_3Dy^{III}_2$	H_6**L34**	5	**2,4M5-1**	75
20	$Cu^{II}_3Dy^{III}_2$	L1, **L3**	5	**2,3,4M5-2**	53
21	$Cu^{II}_3Dy^{III}_2$	H**L39**	5	**(1,2M3-1)+2(0)**	76
22	$Cu^{II}_4Dy^{III}_2$	H**L4**	6	**4M6-1**	77
23	$Cu^{II}_5Dy^{III}$	H_2**L5**	6	**1,5M6-1**	78
24	$Cu^{II}_5Dy^{III}$	H_2**L6**	6	**1,5M6-1**	60
25	$Cu^{II}_4Dy^{III}_2$	H**L9**, HL**10**	6	**1,2,2M6-1**	79
26	$Cu^{II}_3Dy^{III}_3$	H_2**L5**	6	**(1,5M6-1)+(1,5M6-1)**	80
27	$Cu^{II}_5Dy^{III}_2$	H_3**L11**	7	**3,6M7-1**	26
28	$Cu^{II}_5Dy^{III}_2$	H_2**L48**	7	**3,6M7-1**	75
29	$Cu^{II}_6Dy^{III}$	HL**12**	7	**2,6M7-1**	36

30	$Cu^{II}_4Dy^{III}_4$	H_2**L13**	8	**2M8-1**	27
31	$Cu^{II}_6Dy^{III}_2$	H_4**L48**	8	**8(0)**	48
32	$Cu^{II}_4Dy^{III}_4$	H_4**L49**	8	**8(0)**	75
33	$Cu^{II}_5Dy^{III}_4$	H_3L**14**	9	**4,5,8M9-1**	37
34	$Cu^{II}_6Dy^{III}_3$	H_2**L15**	9	**3,6M9-1**	19
35	$Cu^{II}_6Dy^{III}_3$	H_2**L46**	9	**3,6M9-1**	20
36	$Cu^{II}_2Dy^{III}_7$	H_3**L14**	9	**3,3,4,8M9-1**	38
37	$Cu^{II}_7Dy^{III}_2$	H_2**L16**,H_2**L17**	9	**2,2,4,4M9-1**	39
38	$Cu^{II}_5Dy^{III}_4$	H_4**L49**	9	**9(0)**	81
39	$Cu^{II}_8Dy^{III}_2$	H**L18**	10	**4,5,7M10-1**	40
40	$Cu^{II}_9Dy^{III}_2$	H_3**L44**	11	**1,2,3,4,611M-1**	29
41	$Cu^{II}_9Dy^{III}_2$	H**L19**	11	**2,4,5,8M11-2**	41
42	$Cu^{II}_8Dy^{III}_3$	H_3**L20**	11	**2,3,4M11-1**	42
43	$Cu^{II}_8Dy^{III}_4$	H**L21**	12	**3,6M12-1**	43
44	$Cu^{II}_8Dy^{III}_4$	H**L50**	12	**3,6M12-1**	49
45	$Cu^{II}_6Ln^{III}_6$	H_2**L53**	12	**(2,3M4-1)3**	50
46	$Cu^{II}_{10}Dy^{III}_2$	H_2**L50**	12	**(1,5M6-1)+(1,5M6-1)**	80
47	$Cu^{II}_{10}Dy^{III}_2$	H_2**L51**	12	**(1,5M6-1)+(1,5M6-1)**	82
46	$Cu^{II}_{10}Dy^{III}_2$	H_2**L52**	12	**(1,5M6-1)+(1,5M6-1)**	82
49	$Cu^{II}_6Dy^{III}_6$	H_2**L47**	12	**(1M2-1)6**	24,47
50	$Cu^{II}_4Ln^{III}_9$	H_2**L52**	13	**(3,3,5M12-1)+(0)**	50
51	$Cu^{II}_6Ln^{III}_8$	H_3**L55**	14	**14(0)**	83
52	$Cu^{II}_4Dy^{III}_{12}$	H_3**L14**	16	**3,4,6,8M16-1**	38
53	$Cu^{II}_8Dy^{III}_9$	H_2**L22**	17	**2,2,2,2,4,4,5,6,6M17-1**	44
54	$Cu^{II}_{24}Dy^{III}_8$	**L23**	32	**2,3,5,6,6M32-1**	45
55	$Cu^{II}_{36}Dy^{III}_{24}$	H**L24**	60	**4,4,5,6M60-1**	46
56	$Cu^{II}_3Dy^{III}_2$	**complex (2)**	5	**2,3,4M5-2**	
57	$Cu^{II}_5Dy^{III}_5$	**complex (3)**	10	**1,2,2,3,4,5,5,6,6M10-1**	
58	$Cu^{II}_2Dy^{III}_2$	**complex (4)**	4	**2,3M4-1**	
59	$Cu^{II}_2Dy^{III}_2$	**complex (5)**	4	**2,3M4-1**	
60	$Cu^{II}_2Dy^{III}_2$	**complex (6)**	4	**2,3M4-1**	

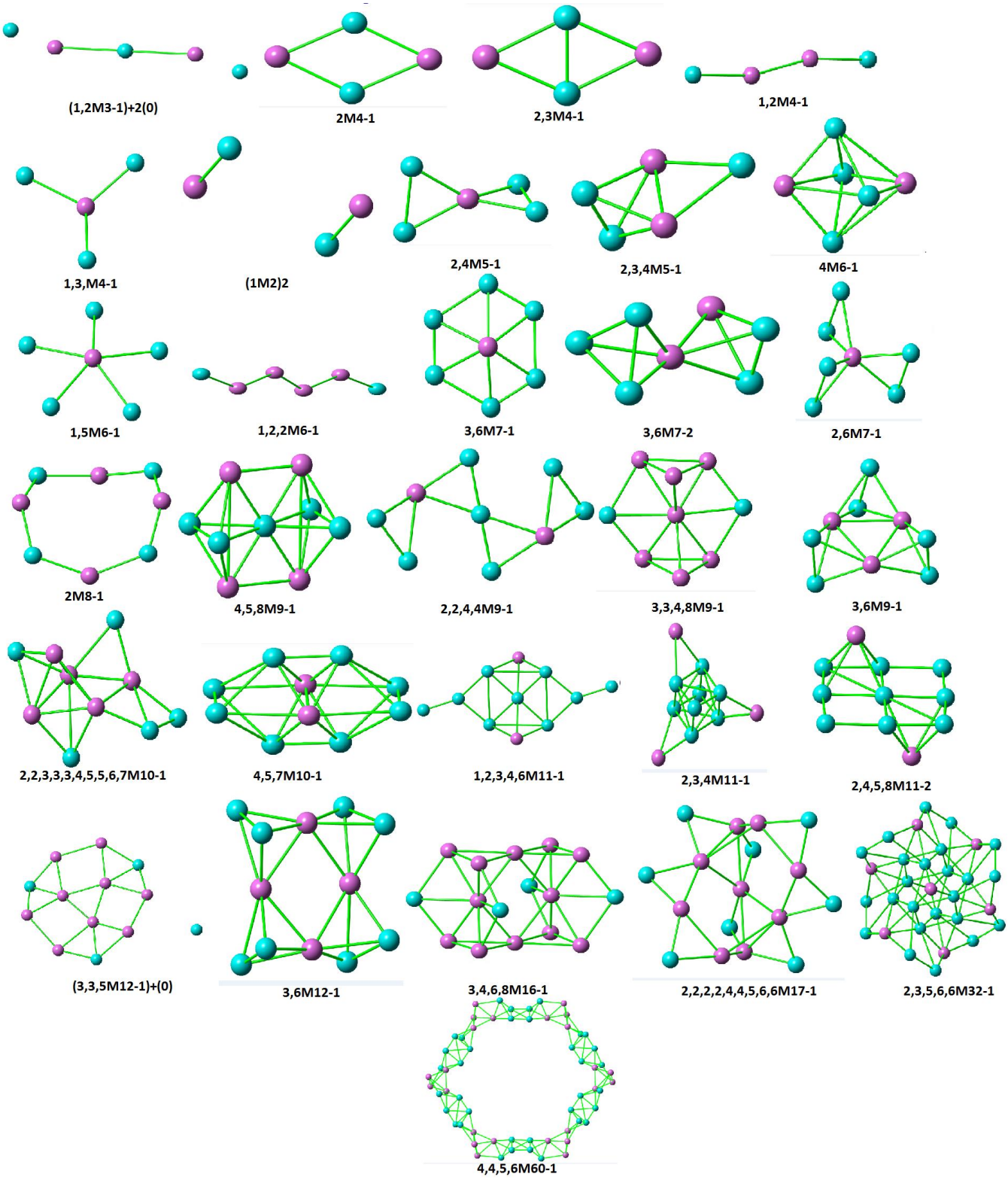

Figure 4. Topological representation of Cu-Dy compounds listed in Table 2.

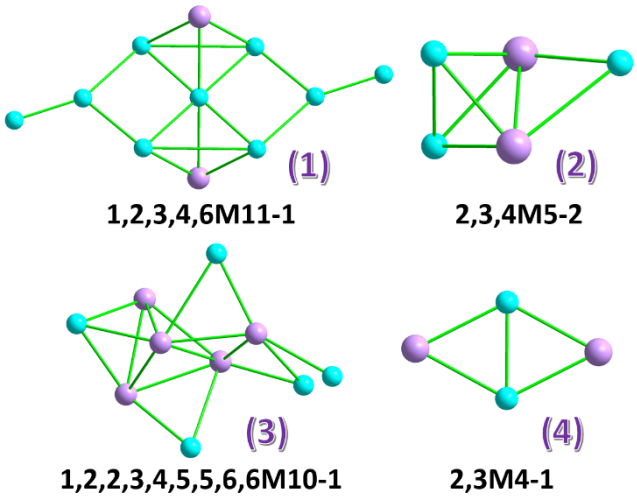

Figure 5. Topological analysis of complex Cu_9Dy_2 (**1**) (top left), Cu_2Dy_3 (**2**) (top right), Cu_5Dy_5 (**3**) (bottom left) and Cu_2Dy_2 (**4**) (bottom right) in comparison. Topological analysis of Cu_2Dy_2 (**4**) is representative for (**5**) and (**6**), respectively.

The topological analysis of Cu_9Dy_2 (**1**) was already published[29] and is **1,2,3,4,6M11-1** shown in Figure 5 and entry number 41 in Table 2. Complex **1** does not show, as expected from the structural analysis, any hint of a relation to a previously described topology within Cu/Dy CCs, or any other topology described here. But we could show that compound **1** is topologically related to a Cu_5Gd_2 compound.[28] While Cu_9Dy_2 can be described as **1,2,3,4,6M11-1**, the pentanuclear complex **2** is described as **2,3,4M5-2** and the decanuclear complex **3** as **1,2,2,3,4,5,5,6,6M10-1**. To the best of our knowledge, **1** and **3** are not related to any structural motif whereas **2** is the second paradigm[53] within the Cu/Dy literature, which is summarized in Table 2. Thus, to the best of our knowledge, whereas **1** forms an extension of the topology previously observed for a Cu_5Gd_2 copound[28] and **2** has the same topology as the previously described Cu_3Dy_2,[53] the topology of **3** is completely new, see Table 2.

As a result of their having the same structural motif, complexes **4** to **6** have the topological description of **2,3M4-1**. This butterfly motif is very common in the literature for all the transition metals and can be found for the Cu/Dy structures in Table 2 as entry number 26, 31, 38.[64,71,84] Although they all have the same topological name, this analysis does not reveal which position is occupied by which metal center. Only the Cu_2Dy_2 structure published by McInnes et al. shows the same metal arrangement as in the case of complex **4** to **6**,[71] with the "body" formed by two Cu^{II} ions and the "wings" by two Dy^{III} ions.

SHAPE Analysis.

It is well known, that the coordination geometry of lanthanide ions has an important influence on the magnetic behavior.[7,11,85] In order to describe the geometries of the lanthanide ions within the structures, they were analyzed using the software SHAPE.[86] The continuous shape measure accompanying each geometry is a measure of how much it deviates from an idealized polyhedron, zero being ideal. The six "best" suggested geometries are given in Table 3 and 4.

Table 3. Results of the SHAPE analysis for the eight-coordinated Dy^{III} ions in complex **2** and **3**.

	CU-8	SAPR-8	TDD-8	JBTPR-8	BTPR-8	JSD-8
Dy(1) [**2**]	11.254	1.038	1.736	1.843	1.648	3.597
Dy(1) [**3**]	12.579	2.033	2.765	2.554	1.503	4.597
Dy(2) [**3**]	11.573	2.563	2.211	3.240	2.938	4.071
Dy(3) [**3**]	10.294	3.829	1.266	3.386	3.337	3.055
Dy(4) [**3**]	14.156	4.394	2.472	3.318	2.740	3.963
Dy(5) [**3**]	8.606	3.576	1.014	3.192	2.466	3.524

Table 4. Results of the SHAPE analysis for the nine-coordinated Dy^{III} ions in complex **1, 2** and **4**.

	MFF-9	CCU-9	JCSAPR-9	CSAPR-9	JTCTPR-9	TCTPR-9
Dy(1) [**1**]	1.285	8.048	2.212	1.261	3.827	2.234
Dy(2) [**2**]	1.327	9.657	1.778	1.434	2.750	1.238
Dy(1) [**4**]	1.896	7.921	3.471	2.064	3.534	1.964

The best polyhedron for both Dy^{III} ions (Dy(1) and Dy(1')) in Cu_9Dy_2 (**1**) are described as capped square antiprisms (1.26%), as highlighted in Figure 6, although a muffin geometry is also very close (1.28%) (see Table 4). The two Dy^{III} ions (Dy(1) and Dy(1')) in Cu_2Dy_2 (**4**) however are approximated as muffin conformation with a very close deviation for being tricapped trigonal prismatic, due to the two coordinating nitrate anions, see Figure 6. The coordination environment for the Dy^{III} ions of compounds **5** and **6** due to their similarity to **4** will not be shown separately.

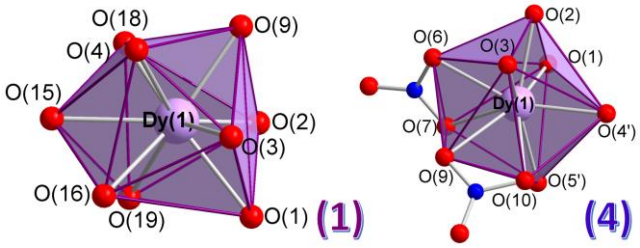

Figure 7. Coordination polyhedron surrounding Dy(1), leading to a capped square antiprism in Cu_9Dy_2 (**1**) (left) and a muffin-shaped surrounding Dy(1) in Cu_2Dy_2 (**4**) (right).

The two Dy^{III} ions (Dy(1) and Dy(2)) in the Cu_3Dy_2 complex (**2**), are obviously different from just a first look at the structure. While Dy(1) exhibits an eight-coordinate environment, Dy(2) has a nine-coordinate ligand sphere, similar to the environments around the Dy^{III} ions in the previously published Cu_3Dy_2 complex.[53] Dy(1) is very close to a square antiprismatic environment, which can also be easily visualized from Figure 7, while the shape of Dy(2) is much closer to a tricapped trigonal prism, but again the deviation from a muffin shape is quite small, see Figure 7 and Table 4.

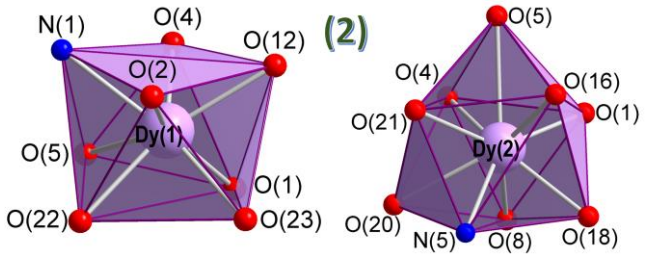

Figure 7. Coordination polyhedron surrounding of the square-antiprismatic Dy(1) (left) and the tricapped trigonal prismatic Dy(2) (right) in Cu_3Dy_2 (**2**).

SHAPE[86] is particularly helpful to estimate the shapes of the coordination polyhedral, especially in the complicated Cu_5Dy_5 (**3**) structure with its different ligand environments, but all being surrounded by eight coordinating atoms. Although there is still a deviation between 1.01-2.47%, Dy(2)-Dy(5) (see Table 3) all four show a triangular dodecahedral environment (see Figure 8), with Dy(3) and Dy(5) showing a deviation less than 1.3%. While Dy(4) and Dy(5) are completely surrounded by atoms provided from Schiff base ligands, Dy(1) needs a coordinating methanol molecule, O(43) to complete its coordination sphere, and similarly Dy(2) and Dy(3) are coordinated to one further nitrate. Dy(1) approximates better to a biaugmented trigonal prismatic coordination sphere, with 1.5% deviation from the perfect shape (Table 4), which is highlighted in Figure 8 in a slightly paler purple to emphasize the difference.

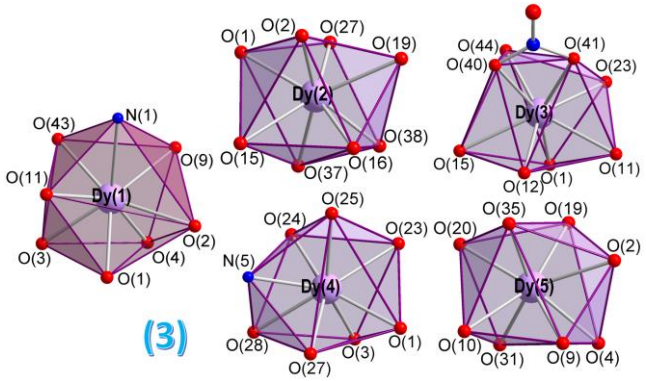

Figure 6. Coordination polyhedra surrounding the five Dy^{III} ions in Cu_5Dy_5 (**3**), with Dy(1) highlighted in a slightly paler purple. The Dy polyhedra for Dy(6) to Dy(10) in cluster 2 are very similar.

For completeness, the coordination environment around each Cu^{II} ion within complexes **1** to **4** will also be described here. The environment of the Cu^{II} ions within complex **1** have been described elsewhere.[29] The results of the SHAPE[86] analysis are shown in Table S4, see ESI. In the asymmetric complex **2** all three Cu^{II} ions show different coordination polyhedra (see Figure 10). Cu(1) has a 4 + 2 distorted octahedral coordination sphere with oxygen atoms on the elongated Jahn-Teller (JT) axis. This JT axis is additionally bent to one side, leading to a deviation from a perfect octahedron of 6.7%. Although Cu(2) and Cu(3) have both five coordinating atoms around them, they show very different coordination polyhedra. While Cu(2) shows a distorted trigonal-bipyramidal environment (deviation from the perfect trigonal-bipyramidal environment of 4.1%), Cu(3) exhibits a square-pyramidal shape with an elongated bond to the bromide ion in the axial position (deviation 3.3%).

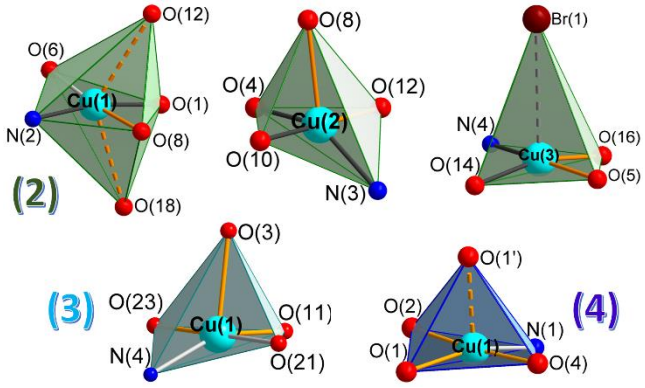

Figure 9. Coordination polyhedra surrounding the different Cu^{II} ions in Cu_3Dy_2 (**2**) (top line), in Cu_5Dy_5 (**3**) (bottom left) and Cu_2Dy_2 (**4**) (bottom right) (square-planar coordination environments are shown in Figure S1 (see ESI)).

In the case of Cu_5Dy_5 (**3**), four out of five Cu^{II} ions exhibit a square-planar environment (see ESI, Figure S1), with the deviation from the perfect square of 0.840% for Cu(2), 0.298% for Cu(3), 0.258% for Cu(4) and 0.245% for Cu(5), approximated with SHAPE.[86] Only Cu(1), which is part of the pseudo-cube with Dy(1), Dy(3) and Dy(4) shows a different environment and approximates better to a square-pyramid, but still shows a deviation of 2.8% from the perfect environment (see Figure 10). All Cu^{II} ions within the complex are surrounded by one ligand and incorporated into pocket 1, defined by the phenoxo oxygen and the imine nitrogen and one diol oxygen, so that 75% of the square-planar environment of Cu(2) to Cu(4) is already provided. In the case of Cu(1) the ligand pocket consists of N(4), O(21) and O(23), see Figure 2 and 10, occupying the equatorial positions.

Both Cu^{II} ions within Cu_2Dy_2 (4) are equivalent due to the inversion center within the molecule. Their polyhedral approximate to a square-pyramidal environment, where the axial bond is slightly elongated, leading to a deviation from the perfect square-pyramid of 2.2%.

Magnetic Properties.

Magnetic susceptibilities of polycrystalline samples of all compounds were measured and will be described here. The temperature dependence of χT for compounds **2**-**4** are shown in Figure 10.

The magnetic data of Cu_9Dy_2 (**1**) are already published,[29] but for completeness the magnetic behavior will be briefly described here.Cu_9Dy_2 (**1**) shows dominant ferromagnetic interactions as seen from the shape of the $\chi_M T$ vs. T plot, leading to a ferrimagnetic spin topology amongst the metal centers. From the AC susceptibility measurements and fits of the Cole-Cole plot, the energy

barrier of this SMM was fitted with the help of the Arrhenius equation leading to U_{eff} = 16.1 K and $\tau_0 = 3.6 \cdot 10^{-7}$ s (R = 0.99).

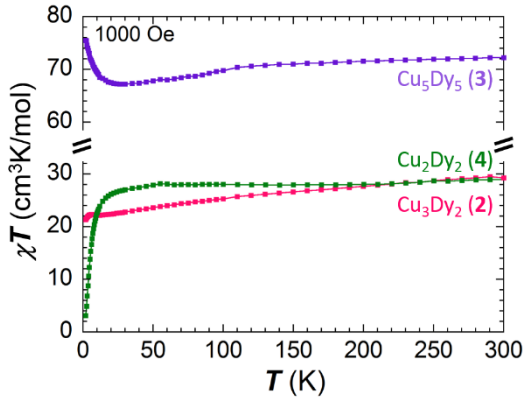

Figure 10. Temperature dependence of the $\chi_M T$ product at 1000 Oe for Cu_3Dy_2 (**2**) (pink), Cu_5Dy_5 (**3**) (purple) and Cu_2Dy_2 (**4**) (green).

The static (dc) magnetic properties for Cu_3Dy_2 (**2**), Cu_5Dy_5 (**3**) and Cu_2Dy_2 (**4**) were studied between 1.9 and 300 K under an applied field of 1000 Oe (Figure 11). The $\chi_M T$ value of 29.3 cm^3K/mol at room temperature for **2** is in good agreement with what is expected for three non-interacting Cu^{II} (S = ½, g = 2, C = 0.375 cm^3K/mol) and two Dy^{III} (S = 5/2, $^6H_{15/2}$, g = 4/3, C = 14.17 cm^3K/mol) ions (29.5 cm^3K/mol). Upon lowering the temperature, the $\chi_M T$ product decreases until it reaches a plateau between 12.0 to 6.0 K with a value of 22.3 cm^3K/mol value. Upon further cooling, the $\chi_M T$ value continuously decreases to reach a value of 21.3 cm^3K/mol at 1.9 K.

In the case of Cu_5Dy_5 (**3**) the $\chi_M T$ product of 72.2 cm^3K/mol at room temperature is in good agreement with the expected value of 72.7 cm^3K/mol for five non-interacting Cu^{II} and five non-interacting Dy^{III} ions (Figure 11). On lowering the temperature, the $\chi_M T$ product of **3** decreases steadily until it reaches the minimum value of 67.2 cm^3K/mol at 28 K. On further cooling, the $\chi_M T$ value sharply increases to reach a value of 75.5 cm^3K/mol at 1.9 K. This behavior is indicative of ferromagnetic interactions between the metal ions.

In case of Cu_2Dy_2 (**4**) the $\chi_M T$ product at high temperature is practically constant upon cooling at a value of 28.1 cm^3K/mol (Figure 11) which is in line with the expected value for two Cu^{II} and two Dy^{III} uncoupled ions (29.1 cm^3K/mol). The sharp decrease below 26 K in the $\chi_M T$ values can be attributed to the combined effect of ligand-field splitting, antiferromagnetic interactions and Zeeman saturation effects. By plotting the $\chi_M T$ product against a logarithmic temperature scale (Figure S2, ESI), it becomes more obvious that the $\chi_M T$ product is heading towards 0 on lowering the temperature which is indicative of a spin ground state of S = 0.

Kahn et al.[87] concluded that in Cu^{II}-Ln^{III} clusters containing a Ln^{III} ion with the $4f^1$-$4f^6$ configuration, a parallel alignment of the spin momenta would lead to an antiparallel alignment of the angular momenta, leading to an overall antiferromagnetic interaction, while for the Ln^{III} ions with the $4f^8$-$4f^{13}$ configurations a parallel alignment of the spin momenta would result in an overall ferromagnetic interaction. This was synthetically shown in literature for dimeric Schiff base complexes based on *o*-vanillin containing one Cu^{II} ion in pocket 1 and one Dy^{III} ion in pocket 2 (according Scheme 1), where the metal centers are ferromagnetically coupled.[21,68,88–93] Cu_2Dy_2 (**4**) is built up from two dimeric Cu^{II}-Dy^{III} units which are linked together through the central Cu^{II} dimer. If both Cu^{II}-Dy^{III} units are ferromagnetically coupled, as seen in in the literature for several compounds,[21,68,88–93] the coupling between these two dimeric units must be strongly antiferromagnetic, to explain the observed $\chi_M T$ product (Figure 11).

Field dependence of magnetization was measured between 2.0 and 5.0 K and the plots are shown in Figure S3 for complex **2** and **3**. In the case of Cu_3Dy_2 (**2**) and Cu_5Dy_5 (**3**), the lack of saturation in the magnetization values indicates the presence of significant magnetic anisotropy and/or low-lying excited states. The values of the isotherms rapidly increase at low field before following a more gradual linear increase after 1.0 T without saturation reaching at 7.0 T and 2.0 K a value of 11.3 μ_B for **2** and a value of 31.0 μ_B for **3**. The anisotropy present in both compounds can be seen from the reduced magnetization plots shown as M vs. H/T (see Figure S2, ESI) which clearly do not superpose on to a single master curve.

For compound **4**, the Cu_2Dy_2 butterfly, the field dependence of magnetization was measured between 2.0 and 5.0 K and the plots are shown in Figure S3. The different isotherms show no saturation up to 7.0 T, but exhibit an S-shaped profile, especially in the 2.0 K isotherm, which is indicative for slow magnetic relaxation and/or presence of a transition between to different magnetic states. For the higher temperature isotherms, the values rapidly increase at small fields before following a more gradual linear increase after 1.0 T without clear saturation. This S-shaped curve progression made us have a closer look into the first derivative of the magnetization curves with respect to the applied field, see Figure S4, ESI. In the 2.0 K isotherm a clear maximum is visible at 1.0 T, indicating a likely presence of a transition between to different magnetic states.[27]

In order to investigate the presence of slow relaxation of the magnetization which may originate from SMM behavior, ac magnetic susceptibility measurements were performed on Cu_3Dy_2 (**2**), Cu_5Dy_5 (**3**) and Cu_2Dy_2 (**4**). In attempts to suppress any quantum tunneling of the magnetization (QTM), the frequency-dependent ac susceptibility was measured with varying applied field (Figure S5 to S7). The in-phase and out-of-phase ac susceptibility of Cu_3Dy_2 (**2**) shows field-dependent signals, but the optimum field could not be established (see Figure S5, ESI). In the case of Cu_5Dy_5 (**3**), the out-of phase susceptibility shows field-dependent signals. Although the maximum could not be found within the measurable frequency window, it is clear that the optimum field where the QTM is smallest is at 500 Oe (see Figure S6, ESI). For the Cu_2Dy_2 complex, **4**, clear maxima were observed, and the optimum field where the

quantum tunneling is smallest was found to be 1500 Oe for Cu_2Dy_2 (**4**) (see Figure S7, ESI).

For complex **3**, ac measurements were carried out under an applied field of 500 Oe and the out-of-phase susceptibility signal is shown in Figure 11 (see Figure S8, ESI). In this case, the out-of-phase signal displays temperature-dependence with no peaks observed within the measurable frequency window and therefore cannot be analyzed with an Arrhenius fit.

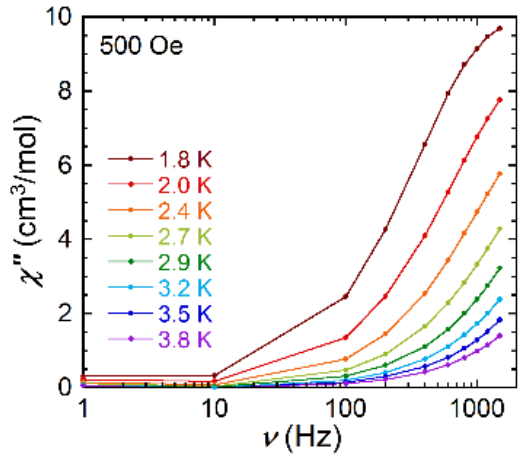

Figure 11. Frequency dependence of the out-of-phase susceptibility of Cu_5Dy_5 (**3**) under a 1500 Oe field in a temperature range between 2.0 and 4.0 K.

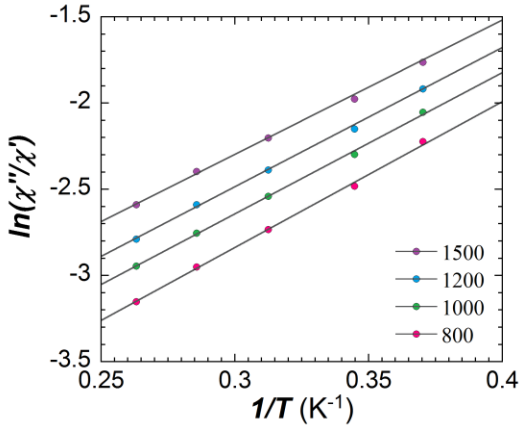

Figure 12. Plot of ln(χ''/χ') versus 1/T for the Cu_5Dy_5 complex **3**. The grey solid lines represent the fitted results over the range of 800 - 1500 Hz and 2.4 - 3.8 K (bottom).

We then used the method proposed by Bartolomé et al.[94,95] to estimate the energy barrier and the characteristic relaxation time. This method is based on the assumption that there is only one relaxation process of the Debye type, and U_{eff} and τ_0 are given by $\ln(\chi''/\chi') = \ln(\omega\tau_0) + U_{eff}/k_BT$, which is based on the Kramers-Kronig equation.[94,95] We have used the χ' and χ'' at high frequencies (ν = 1500, 1200, 1000 and 800 Hz) and at different temperature values (T = 2.7, 2.9, 3.2, 3.5 and 3.8 K) to construct a ln(χ''/χ') vs 1/T plot (see Figure 12), where ω (= 2πν) is the angular frequency of the ac field. Fitting the data for the highest temperature values, leading to almost parallel lines, which indicate one single process in that temperature regime. At lower temperatures, secondary effects such as QTM may also occur. The average of the obtained parameters gave U_{eff} ~ 8.1 K and $\tau_0 \sim 9.7 \cdot 10^{-7}$ s. For further details see Supporting Information, S5.

For the Cu_2Dy_2 complex (**4**), the ac measurements were carried out under a dc field of 1500 Oe and reveal temperature dependent in- and out-of-phase signals over the whole applied temperature range (Figure S9 and Figure 13). The frequency dependent out-of phase susceptibility signals show clear maxima between 2.0 and 2.8 K, see Figure 14, which were used to determine the energy barrier using an Arrhenius fit, Figure 14 (inset), giving U_{eff} = 16.5 K and $\tau_0 = 4.5 \cdot 10^{-7}$ s (R = 0.99).

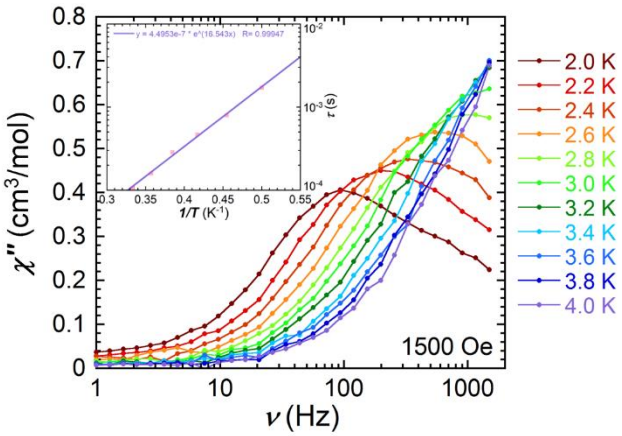

Figure 13. Frequency dependence of the out-of-phase susceptibility of Cu_2Dy_2 (**4**) under a 1500 Oe field in a temperature range between 2.0 and 4.0 K and Arrhenius fit (inset).

Conclusions

In summary, six complexes with three slightly different ligands have been synthesized and characterized. The results show that there is an influence from using different copper sources, leading to the same structural motif when using $Cu(NO_3)_3$, while the use of $CuBr_2$ leads to three structurally unrelated complexes with this set of ligands. Additionally, there is also a steric influence arising from the nature of the alkyl residue on going from HL_2 (methyl) to HL_3 (ethyl). The topological analysis reveals that Cu_9Dy_2 **1** and Cu_5Dy_5 **3** are not related to any structural motif reported so far, whereas **2** is the second example within the Cu/Dy literature. Table 2 gives a summary of all Cu/Dy complexes published so far and can therefore be used as a database. From a topological point of view, complex **1** forms an extension of the topology previously observed for a Cu_5Gd_2 copound[28] and **2** has the same topology as the previously described Cu_3Dy_2,[53] whilst the topology of **3** is completely new. Cu_2Dy_2 **4** shows a well-known butterfly motif. All complexes show frequency-dependent out-of phase ac susceptibility signals, which is an indicator for SMM behavior. Complex **3**, Cu_5Dy_5, displays temperature-dependent out-of-phase signals with no maxima observed within the measurable frequency window, therefore

the method proposed by Bartolomé et al. was used to estimate the energy barrier and the characteristic relaxation time, while in the case of the butterfly structure Cu_2Dy_2, **4**, out-of phase susceptibility signals show clear maxima which were used to determine the energy barrier using an Arrhenius fit.

ASSOCIATED CONTENT

Supporting Information. This material is available free of charge via the Internet at http://pubs.acs.org.
Synthesis, Topos analysis, Shape analysis and magnetic data (PDF).
Crystallographic data for the structures in this paper have been deposited with the Cambridge Crystallographic Data Centre as supplementary publication nos. CCDC 1548219-1548223. Copies of the data can be obtained, free of charge, from https://summary.ccdc.cam.ac.uk/structure-summary-form.
Crystallographic details in CIF format (CIF).

AUTHOR INFORMATION

Corresponding Author

* Email: annie.powell@kit.edu
* Email: g.kostakis@sussex.ac.uk

Present Addresses

† School of Chemistry and Chemical Biology, University College Dublin (UCD), Belfield, Dublin 4, Ireland.

Author Contributions

The manuscript was written through contributions of all authors. / All authors have given approval to the final version of the manuscript.

Funding Sources

We acknowledge DFG (SFB/TRR 88 - 3MET) and the Helmholtz Gemeinschaft POF STN for funding. I.A.K. thanks the Karlsruhe House of Young Scientists (KHYS) for funding the research stay at the University of Sussex, UK, to start this collaboration, and also the Irish Research Council (IRC) for the GOIDP fellowship. G.E.K. acknowledges the University of Sussex for offering a PhD position to K.G. and O.P.E.T. is grateful for Summer Fellowship from the University of Sussex.

Notes

The authors declare no competing financial interest.

ACKNOWLEDGMENT

We acknowledge Dr. Abhishake Mondal and Dr. Valeriu Mereacre for collecting the magnetic data and Lena Friedrich for assistance with synthetic work. G.E.K. acknowledges the University of Sussex for offering a PhD position to K. G. We thank the EPSRC UK National Crystallography Service at the University of Southampton[59] for the collection of the crystallographic data for compound **3, 4** and **4'**,

REFERENCES

(1) Sessoli, R.; Gatteschi, D.; Caneschi, A.; Novak, M. A. Magnetic Bistability in a Metal-Ion Cluster. *Nature* **1993**, *365*, 141–143 DOI: 10.1038/365141a0.

(2) Villain, J.; Hartman-Boutron, F.; Sessoli, R.; Rettori, A. Magnetic Relaxation in Big Magnetic Molecules. *Europhys. Lett.* **1994**, *27*, 159–164 DOI: 10.1209/0295-5075/27/2/014.

(3) Bogani, L.; Wernsdorfer, W. Molecular Spintronics Using Single-Molecule Magnets. *Nat. Mater.* **2008**, *7*, 179–186 DOI: 10.1038/nmat2133.

(4) Vincent, R.; Klyatskaya, S.; Ruben, M.; Wernsdorfer, W.; Balestro, F. Electronic Read-out of a Single Nuclear Spin Using a Molecular Spin Transistor. *Nature* **2012**, *488*, 357–360 DOI: 10.1038/nature11341.

(5) Kahn, M. L.; Sutter, J. P.; Golhen, S.; Guionneau, P.; Ouahab, L.; Kahn, O.; Chasseau, D. Systematic Investigation of the Nature of the Coupling between a Ln(III) Ion (Ln = Ce(III) to Dy(III)) and Its Aminoxyl Radical Ligands. Structural and Magnetic Characteristics of a Series of {Ln(organic radical)2} Compounds and the Related {Ln(Nitrone)2}. *J. Am. Chem. Soc.* **2000**, *122*, 3413–3421 DOI: 10.1021/ja9941750.

(6) Sessoli, R.; Powell, A. K. Strategiies towards Single Molecule Magnets. *Coord. Chem. Rev.* **2009**, *253*, 2328–2341.

(7) Sorace, L.; Benelli, C.; Gatteschi, D. Lanthanides in Molecular Magnetism: Old Tools in a New Field. *Chem. Soc. Rev.* **2011**, *40*, 3092 DOI: 10.1039/c0cs00185f.

(8) Wernsdorfer, W.; Aliaga-Alcalde, N.; Hendrickson, D. N.; Christou, G. Exchange-Biased Quantum Tunnelling in a Supramolecular Dimer of Single-Molecule Magnets. *Nature* **2002**, *416*, 406–409 DOI: 10.1038/416406a.

(9) Christou, G.; Gatteschi, D.; Hendrickson, D. N.; Sessoli, R. Single-Molecule Magnets. *MRS Bull.* **2000**, *25*, 66–71 DOI: 10.1557/mrs2000.226.

(10) Tasiopoulos, A. J.; Vinslava, A.; Wernsdorfer, W.; Abboud, K. A.; Christou, G. Giant Single-Molecule Magnets: A{Mn84} Torus and Its Supramolecular Nanotubes. *Angew. Chem.* **2004**, *116*, 2169–2173 DOI: 10.1002/ange.200353352.

(11) Rinehart, J. D.; Long, J. R. Exploiting Single-Ion Anisotropy in the Design of F-Element Single-Molecule Magnets. *Chem. Sci.* **2011**, *2*, 2078–2085 DOI: 10.1039/C1SC00513H.

(12) Novitchi, G.; Pilet, G.; Ungur, L.; Moshchalkov, V. V.; Wernsdorfer, W.; Chibotaru, L. F.; Luneau, D.; Powell, A. K. Heterometallic CuII/DyIII 1D Chiral Polymers: Chirogenesis and Exchange Coupling of Toroidal Moments in Trinuclear Dy3 Single Molecule Magnets. *Chem. Sci.* **2012**, *3*, 1169 DOI: 10.1039/c2sc00728b.

(13) Novitchi, G.; Wernsdorfer, W.; Chibotaru, L. F.; Costes, J.-P.; Anson, C. E.; Powell, A. K. Supramolecular "double-Propeller" dimers of Hexanuclear Cu(II)/Ln(III) Complexes: A {Cu3Dy3}2 Single-Molecule Magnet. *Angew. Chem. Int. Ed.* **2009**, *48*, 1614–1619 DOI: 10.1002/anie.200805176.

(14) Langley, S. K.; Ungur, L.; Chilton, N. F.; Moubaraki, B.; Chibotaru, L. F.; Murray, K. S. Structure, Magnetism and Theory of a Family of Nonanuclear Cu II5LnIII4-Triethanolamine Clusters Displaying Single-Molecule Magnet Behaviour. *Chem. - A Eur. J.* **2011**, *17*, 9209–9218 DOI: 10.1002/chem.201100218.

(15) Iasco, O.; Novitchi, G.; Jeanneau, E.; Wernsdorfer, W.; Luneau, D. Benzoxazole-Based Heterometallic Dodecanuclear Complex $[Dy^{III}_4Cu^{II}_8]$ with Single-Molecule-Magnet Behavior. *Inorg. Chem.* **2011**, *50*, 7373–7375 DOI: 10.1021/ic201070n.

(16) Osa, S.; Kido, T.; Matsumoto, N.; Re, N.; Pochaba, A.; Mrozinski, J. A Tetranuclear 3d-4f Single Molecule Magnet: [CuIILTbIII(hfac)2]2. *J. Am. Chem. Soc.* **2004**, *126*, 420–421 DOI: 10.1021/ja037365e.

(17) Baskar, V.; Gopal, K.; Helliwell, M.; Tuna, F.; Wernsdorfer, W.; Winpenny, R. E. P. Magnetic Quantum Tunneling: Insights from Simple Molecule-Based Magnets. *Dalton Trans.* **2010**, *39*, 4693 DOI: 10.1039/c002750b.

(18) Mori, F.; Nyui, T.; Ishida, T.; Nogami, T.; Choi, K.-Y.; Nojiri, H. Oximate-Bridged Trinuclear Dy-Cu-Dy Complex Behaving as a Single-Molecule Magnet and Its Mechanistic Investigation. *J. Am. Chem. Soc.* **2006**, *128*, 1440–1441 DOI: 10.1021/ja057183f.

(19) Aronica, C.; Pilet, G.; Chastanet, G.; Wernsdorfer, W.; Jacquot, J.-F. F.; Luneau, D. A Nonanuclear Dysprosium(III)–

Copper(II) Complex Exhibiting Single-Molecule Magnet Behavior with Very Slow Zero-Field Relaxation. *Angew. Chem. Int. Ed.* **2006**, *45*, 4659–4662 DOI: 10.1002/anie.200600513.

(20) Modak, R.; Sikdar, Y.; Cosquer, G.; Chatterjee, S.; Yamashita, M.; Goswami, S. Heterometallic CuII-DyIII Clusters of Different Nuclearities with Slow Magnetic Relaxation. *Inorg. Chem.* **2016**, 55, 691–699 DOI: 10.1021/acs.inorgchem.5b02107.

(21) Kajiwara, T.; Nakano, M.; Takahashi, K.; Takaishi, S.; Yamashita, M. Structural Design of Easy-Axis Magnetic Anisotropy and Determination of Anisotropic Parameters of Ln^{III}-Cu^{II} Single-Molecule Magnets. *Chem. - A Eur. J.* **2011**, *17*, 196–205 DOI: 10.1002/chem.201002434.

(22) Kajiwara, T.; Takahashi, K.; Hiraizumi, T.; Takaishi, S.; Yamashita, M. Structural Correlations between the Crytsal Field and Magnetic Anisotropy of Ln-Cu Single-Molecule Magnets. *Cryst. Eng. Commun.* **2009**, *11*, 2117–2120 DOI: 10.1039/b905912a.

(23) Iasco, O.; Novitchi, G.; Jeanneau, E.; Luneau, D. Lanthanide Triangles Sandwiched by Tetranuclear Copper Complexes Afford a Family of Hendecanuclear Heterometallic Complexes $[Ln^{III}_3Cu^{II}_8]$ (Ln = La–Lu): Synthesis and Magnetostructural Studies. *Inorg. Chem.* **2013**, *52*, 8723–8731 DOI: 10.1021/ic4009015.

(24) Dinca, A. S.; Ghirri, A.; Madalan, A. M.; Affronte, M.; Andruh, M. Dodecanuclear $[Cu_6Gd_6]$ Nanoclusters as Magnetic Refridgerants. *Inorg. Chem.* **2012**, *51*, 3935–3937.

(25) Xue, S.; Guo, Y. N.; Zhao, L.; Zhang, H.; Tang, J. Molecular Magnetic Investigation of a Family of Octanuclear $[Cu_6Ln_2]$ Nanoclusters. *Inorg. Chem.* **2014**, 53, 8165–8171 DOI: 10.1021/ic501226v.

(26) Chandrasekhar, V.; Dey, A.; Das, S.; Rouzières, M.; Clérac, R. Syntheses, Structures, and Magnetic Properties of a Family of Heterometallic Heptanuclear [Cu5Ln2] (Ln = Y(III), Lu(III), Dy(III), Ho(III), Er(III), and Yb(III)) Complexes: Observation of SMM Behavior for the Dy(III) and Ho(III) Analogues. *Inorg. Chem.* **2013**, 52, 2588–2598 DOI: 10.1021/ic302614k.

(27) Kühne, I. A.; Magnani, N.; Mereacre, V.; Wernsdorfer, W.; Anson, C. E.; Powell, A. K. An Octanuclear {CuII4DyIII4} Coordination Cluster Showing Single Molecule Magnet Behaviour from Field Accessible States. *Chem. Commun.* **2014**, *50*, 1882 DOI: 10.1039/c3cc46458j.

(28) Wu, G.; Hewitt, I. J.; Mameri, S.; Lan, Y.; Clérac, R.; Anson, C. E.; Qiu, S.; Powell, A. K. Bifunctional Ligand Approach for Constructing 3d-4f Heterometallic Clusters. *Inorg. Chem.* **2007**, *46*, 7229–7231 DOI: 10.1021/ic070296a.

(29) Kühne, I. A.; Kostakis, G. E.; Anson, C. E.; Powell, A. K. An Undecanuclear Ferrimagnetic Cu 9 Dy 2 Single Molecule Magnet Achieved through Ligand Fine-Tuning. *Inorg. Chem.* **2016**, 55, 4072–4074 DOI: 10.1021/acs.inorgchem.6b00490.

(30) Hathaway, B. J. Copper. *Coord. Chem. Rev.* **1981**, *35* (C), 211–252 DOI: 10.1016/S0010-8545(00)80463-4.

(31) Nishida, Y.; Kida, S. Splitting of D-Orbitals in Square Planar Complexes of copper(II), nickel(II) and cobalt(II). *Coord. Chem. Rev.* **1979**, *27*, 275–298 DOI: 10.1016/S0010-8545(00)82069-X.

(32) Baskar, V.; Gopal, K.; Helliwell, M.; Tuna, F.; Wernsdorfer, W.; Winpenny, R. E. P. 3d-4f Clusters with Large Ground States and SMM Behaviour. *Dalton Trans.* **2010**, *39*, 4747–4750 DOI: 10.1039/c002750b.

(33) Andruh, M.; Costes, J. P.; Diaz, C.; Gao, S. 3D-4F Combined Chemistry: Synthetic Strategies and Magnetic Properties. *Inorg. Chem.* **2009**, *48*, 3342–3359 DOI: 10.1021/ic801027q.

(34) Feltham, H. L. C.; Cl??rac, R.; Powell, A. K.; Brooker, S. A Tetranuclear, Macrocyclic 3d-4f Complex Showing Single-Molecule Magnet Behavior. *Inorg. Chem.* **2011**, *50*, 4232–4234 DOI: 10.1021/ic2003639.

(35) Andruh, M. Compartmental Schiff-Base Ligands-a Rich Library of Tectons in Designing Magnetic and Luminescent Materials. *Chem. Commun.* **2011**, *47*, 3025 DOI: 10.1039/c0cc04506c.

(36) Sopasis, G. J.; Canaj, A. B.; Philippidis, A.; Siczek, M.; Lis, T.; O'Brien, J. R.; Antonakis, M. M.; Pergantis, S. A.; Milios, C. J. Heptanuclear Heterometallic $[Cu_6Ln]$ Clusters: Trapping Lanthanides into Copper Cages with Artificial Amino Acids. *Inorg. Chem.* **2012**, *51*, 5911–5918 DOI: 10.1021/ic300538q.

(37) Langley, S. K.; Ungur, L.; Chilton, N. F.; Moubaraki, B.; Chibotaru, L. F.; Murray, K. S. Structure, Magnetism and Theory of a Family of Nonanuclear Cu(II)5Ln(III)4-Triethanolamine Clusters Displaying Single-Molecule Magnet Behaviour. *Chem. Eur. J.* **2011**, *17*, 9209–9218 DOI: 10.1002/chem.201100218.

(38) Langley, S. K.; Moubaraki, B.; Tomasi, C.; Evangelisti, M.; Brechin, E. K.; Murray, K. S. Synthesis, Structure, and Magnetism of a Family of Heterometallic {Cu2Ln7} and {Cu4Ln12} (Ln = Gd, Tb, and Dy) Complexes: The Gd Analogues Exhibiting a Large Magnetocaloric Effect. *Inorg. Chem.* **2014**, 53, 13154–13161 DOI: 10.1021/ic5023467.

(39) Liu, J.-L.; Chen, Y.-C.; Li, Q.-W.; Gómez-Coca, S.; Aravena, D.; Ruiz, E.; Lin, W.-Q.; Leng, J.-D.; Tong, M.-L. Two 3d–4f Nanomagnets Formed via a Two-Step in Situ Reaction of Picolinaldehyde. *Chem. Commun.* **2013**, *49*, 6549 DOI: 10.1039/c3cc43200a.

(40) Borta, A.; Jeanneau, E.; Chumakov, Y.; Luneau, D.; Ungur, L.; Chibotaru, L. F.; Wernsdorfer, W. Synthesis{,} Structure{,} Magnetism and Theoretical Study of a Series of Complexes with a Decanuclear Core [Ln(iii)2Cu(ii)8] (Ln = Y{,} Gd{,} Tb{,} Dy). *New J. Chem.* **2011**, *35*, 1270–1279 DOI: 10.1039/C0NJ00931H.

(41) Kuang, W.-W.; Zhu, L.-L.; Li, L.-C.; Yang, P.-P. Synthesis, Crystal Structure, and Magnetic Properties of a Family of Undecanuclear $[Cu^{II}_9 Ln^{III}_2]$ Nanoclusters. *Eur. J. Inorg. Chem.* **2015**, *2015*, 2245–2253 DOI: 10.1002/ejic.201500064.

(42) Iasco, O.; Novitchi, G.; Jeanneau, E.; Luneau, D. Lanthanide Triangles Sandwiched by Tetranuclear Copper Complexes Afford a Family of Hendecanuclear Heterometallic Complexes $[Ln^{III}3Cu^{II}_8]$ (Ln = La–Lu): Synthesis and Magnetostructural Studies. *Inorg. Chem.* **2013**, *52*, 8723–8731 DOI: 10.1021/ic4009015.

(43) Iasco, O.; Novitchi, G.; Jeanneau, E.; Wernsdorfer, W.; Luneau, D. Benzoxazole-Based Heterometallic Dodecanuclear Complex $[Dy^{III}4Cu^{II}_8]$ with Single-Molecule-Magnet Behavior. *Inorg. Chem.* **2011**, *50*, 7373–7375 DOI: 10.1021/ic201070n.

(44) Liu, J.-L.; Lin, W.-Q.; Chen, Y.-C.; Gómez-Coca, S.; Aravena, D.; Ruiz, E.; Leng, J.-D.; Tong, M.-L. CuII-GdIII Cryogenic Magnetic Refrigerants and Cu_8Dy9 Single-Molecule Magnet Generated by In Situ Reactions of Picolinaldehyde and Acetylpyridine: Experimental and Theoretical Study. *Chem. - A Eur. J.* **2013**, *19*, 17567–17577 DOI: 10.1002/chem.201303275.

(45) Baskar, V.; Gopal, K.; Helliwell, M.; Tuna, F.; Wernsdorfer, W.; Winpenny, R. E. P. 3d-4f Clusters with Large Spin Ground States and SMM Behaviour. *Dalton Trans.* **2010**, *39*, 4747–4750 DOI: 10.1039/b927114g.

(46) Hamamatsu, T.; Yabe, K.; Towatari, M.; Matsumoto, N.; Re, N.; Pochaba, A.; Mrozinski, J. Synthesis and Magnetic Property of Copper(II)–Lanthanide(III) Complexes [{CuIILLnIII (O-van)(CH3COO)(MeOH)} 2]·2H2O. *Bull. Chem. Soc. Jpn.* **2007**, *80*, 523–529 DOI: 10.1246/bcsj.80.523.

(47) Dinca, A. S.; Shova, S.; Ion, A. E.; Maxim, C.; Lloret, F.; Julve, M.; Andruh, M. Ascorbic Acid Decomposition into Oxalate Ions: A Simple Synthetic Route towards Oxalato-Bridged Heterometallic 3d–4f Clusters. *Dalton Trans.* **2015**, *44*, 7148–7151 DOI: 10.1039/C5DT00778J.

(48) Wu, J.; Zhao, L.; Guo, M.; Tang, J. Constructing Supramolecular Grids: From 4f Square to 3d-4f Grid. *Chem. Commun.* **2015**, *51*, 17317–17320 DOI: 10.1039/c5cc06960b.

(49) Joarder, B.; Mukherjee, S.; Patil, M.; Xue, S.; Tang, J.; Ghosh, S. K. Chiral Biomolecule Based Dodecanuclear Dysprosium(Iii)–copper(Ii) Clusters: Structural Analyses and Magnetic

Properties. *Inorg. Chem. Front.* **2015**, *2*, 854–859 DOI: 10.1039/C5QI00090D.

(50) Moreno Pineda, E.; Heesing, C.; Tuna, F.; Zheng, Y.-Z.; McInnes, E. J. L.; Schnack, J.; Winpenny, R. E. P. Copper Lanthanide Phosphonate Cages: Highly Symmetric {Cu3Ln9P6} and {Cu6Ln6P6} Clusters with C3v and D3h Symmetry. *Inorg. Chem.* **2015**, *54*, 6331–6337 DOI: 10.1021/acs.inorgchem.5b00649.

(51) Chopin, N.; Novitchi, G.; Médebielle, M.; Pilet, G. A Versatile Ethanolamine-Derived Trifluoromethyl Enaminone Ligand for the Elaboration of nickel(II) and copper(II)–dysprosium(III) Multinuclear Complexes with Magnetic Properties. *J. Fluor. Chem.* **2015**, *179*, 169–174 DOI: 10.1016/j.jfluchem.2015.06.023.

(52) Kühne, I. A.; Mereacre, V.; Anson, C. E.; Powell, A. K. Nine Members of a Family of Nine-Membered Cyclic Coordination Clusters; Fe 6 Ln 3 Wheels (Ln = Gd to Lu and Y). *Chem. Commun.* **2016**, *52*, 1021–1024 DOI: 10.1039/C5CC08887A.

(53) Escobar, L. B. L.; Guedes, G. P.; Soriano, S.; Speziali, N. L.; Jordão, A. K.; Cunha, A. C.; Ferreira, V. F.; Maxim, C.; Novak, M. A.; Andruh, M.; Vaz, M. G. F. New Families of Hetero-Tri-Spin 2p–3d–4f Complexes: Synthesis, Crystal Structures, and Magnetic Properties. *Inorg. Chem.* **2014**, *53*, 7508–7517 DOI: 10.1021/ic5008044.

(54) Blatov, V. A.; Shevchenko, A. P.; Proserpio, D. M. Applied Topological Analysis of Crystal Structures with the Program Package ToposPro. *Cryst. Growth Des.* **2014**, *14*, 3576–3586 DOI: 10.1021/cg500498k.

(55) Kostakis, G. E.; Blatov, V. A.; Proserpio, D. M. A Method for Topological Analysis of High Nuclearity Coordination Clusters and Its Application to Mn Coordination Compounds. *Dalton Trans.* **2012**, *41*, 4634–4640 DOI: 10.1039/c2dt12263d.

(56) Tasiopoulos, A. J.; Perlepes, S. P. Diol-Type Ligands as Central "players" in the Chemistry of High-Spin Molecules and Single-Molecule Magnets. *Dalton Trans.* **2008**, 5537–5555 DOI: 10.1039/b805014g.

(57) Goura, J.; Chakraborty, A.; Walsh, J. P. S.; Tuna, F.; Chandrasekhar, V. Hexanuclear 3d–4f Neutral Co II 2 Ln III 4 Clusters: Synthesis, Structure, and Magnetism. *Cryst. Growth Des.* **2015**, *15*, 3157–3165 DOI: 10.1021/acs.cgd.5b00588.

(58) Kostakis, G. E. Topological Aspects of 3d/4f Polynuclear Coordination Clusters. In *Elsevier Reference Module in Chemistry, Molecular Sciences and Chemical Engineering*; Reedijk, J., Ed.; Elsevier: Waltham, MA, 2016; pp 1–53.

(59) Tan, X.; Ji, X.; Zheng, J.-M. Heterometallic Tetranuclear 3d–4f Complexes: Syntheses, Structures and Magnetic Properties. *Inorg. Chem. Commun.* **2015**, *60*, 27–32 DOI: 10.1016/j.inoche.2015.07.027.

(60) Blake, A. J.; Cherepanov, V. A.; Dunlop, A. A.; Grant, C. M.; Milne, P. E. Y.; Rawson, J. M.; Winpenny, R. E. P. Synthesis, Crystal Structures and Thermal Decomposition Studies of a Series of Copper–lanthanoid Complexes of 6-Methyl-2-Pyridone. *J. Chem. Soc., Dalton Trans.* **1994**, *67*, 2719–2727 DOI: 10.1039/DT9940002719.

(61) Kajiwara, T.; Takahashi, K.; Hiraizumi, T.; Takaishi, S.; Yamashita, M. Structural Correlations between the Crystal Field and Magnetic Anisotropy of Ln-Cu Single-Molecule Magnets. *CrystEngComm* **2009**, *11*, 2110–2116 DOI: 10.1039/B906182G.

(62) Zemin, Z.; Fusheng, G. U. O.; Penghu, G. U. O.; Junliang, L. I. U. Di- and Tetranuclear Heterometallic Cu II -Ln III Complexes (Ln = Gd and Dy): Synthesis , Structure and Magnetic Properties. **2012**, *55*, 934–941 DOI: 10.1007/s11426-012-4564-3.

(63) Hamamatsu, T.; Yabe, K.; Towatari, M.; Matsumoto, N.; Re, N.; Pochaba, A.; Mrozinski, J. Synthesis and Magnetic Property of Copper(II)–Lanthanide(III) Complexes [{Cu II LLn III (O -van)(CH 3 COO)(MeOH)} 2]·2H 2 O (Ln III = Gd^{III}, Tb^{III}, and Dy^{III} ; H 3 L = 1-(2-Hydroxybenzamido)-2-(2-Hydroxy-3-Methoxybenzylideneamino)ethane; O -van = 3. *Bull. Chem. Soc. Jpn.* **2007**, *80*, 523–529 DOI: 10.1246/bcsj.80.523.

(64) Kettles, F. J.; Milway, V. A.; Tuna, F.; Valiente, R.; Thomas, L. H.; Wernsdorfer, W.; Ochsenbein, S. T.; Murrie, M. Exchange Interactions at the Origin of Slow Relaxation of the Magnetization in {TbCu3} and {DyCu3} Single-Molecule Magnets. *Inorg. Chem.* **2014**, *53*, 8970–8978 DOI: 10.1021/ic500885r.

(65) Costes, J.-P.; Shova, S.; Wernsdorfer, W. Tetranuclear [Cu-Ln]2 Single Molecule Magnets: Synthesis, Structural and Magnetic Studies. *Dalton Trans.* **2008**, 14, 1843–1849 DOI: 10.1039/b716098d.

(66) Tan, X.; Che, Y. X.; Zheng, J. M. Two Tetranuclear 3d-4f Complexes: Syntheses, Structures and Magnetic Properties. *Inorg. Chem. Commun.* **2013**, *37*, 17–20 DOI: 10.1016/j.inoche.2013.09.019.

(67) Wu, J.; Zhao, L.; Zhang, P.; Zhang, L.; Guo, M.; Tang, J. Linear 3d-4f Compounds: Synthesis, Structure, and Determination of the D-F Magnetic Interaction. *Dalton Trans.* **2015**, *44*, 11935–11942 DOI: 10.1039/c5dt01382h.

(68) Zhang, P.; Zhang, L.; Lin, S.-Y.; Tang, J. Tetranuclear [MDy] 2 Compounds and Their Dinuclear [MDy] (M = Zn / Cu) Building Units : The Assembly , Structures and Magnetic Properties. *Inorg. Chem.* **2013**, *52*, 6595–6602.

(69) Feltham, H. L. C.; Clérac, R.; Ungur, L.; Vieru, V.; Chibotaru, L. F.; Powell, A. K.; Brooker, S. Synthesis and Magnetic Properties of a New Family of Macrocyclic M(II)3Ln(III) Complexes: Insights into the Effect of Subtle Chemical Modification on Single-Molecule Magnet Behavior. *Inorg. Chem.* **2012**, *51*, 10603–10612 DOI: 10.1021/ic300819u.

(70) Benelli, C.; Blake, A. J.; Milne, P. E. Y.; Rawson, J. M.; Winpenny, R. E. P. Magnetic and Structural Studies of Copper - Lanthanoid Complexes ; the Synthesis and Structures of New Cu , Ln Complexes of 6-Chloro-Zpyridone (Ln = Gd , Dy and Er) and Magnetic Studies on Cu , Gd ,, Cu , Gd , and Cu , Gd Complexes. *Chem. Eur. J.* **1995**, *1*, 614–618.

(71) Moreno Pineda, E.; Chilton, N. F.; Tuna, F.; Winpenny, R. E. P.; McInnes, E. J. L. Systematic Study of a Family of Butterfly-Like {M2Ln2} Molecular Magnets (M = MgII, MnIII, CoII, NiII, and CuII; Ln = YIII, GdIII, TbIII, DyIII, HoIII, and ErIII). *Inorg. Chem.* **2015**, *54*, 5930–5941 DOI: 10.1021/acs.inorgchem.5b00746.

(72) Kettles, F. J.; Milway, V. A.; Tuna, F.; Valiente, R.; Thomas, L. H.; Wernsdorfer, W.; Ochsenbein, S. T.; Murrie, M. Exchange Interactions at the Origin of Slow Relaxation of the Magnetization in {TbCu3} and {DyCu3} Single-Molecule Magnets. *Inorg. Chem.* **2014**, *53*, 8970–8978 DOI: 10.1021/ic500885r.

(73) Ueki, S.; Ishida, T.; Nogami, T.; Choi, K.-Y.; Nojiri, H. Quantum Tunneling of Magnetization via Well-Defined Dy–Cu Exchange Coupling in a Ferrimagnetic High-Spin [Dy4Cu] Single-Molecule Magnet. *Chem. Phys. Lett.* **2007**, *440*, 263–267 DOI: 10.1016/j.cplett.2007.04.063.

(74) Wang, X.-F.; Hu, P.; Li, Y.-G.; Li, L.-C. Construction of Nitronyl Nitroxide-Based 3d–4f Clusters: Structure and Magnetism. *Chem. – An Asian J.* **2015**, *10*, 325–328 DOI: 10.1002/asia.201403165.

(75) Richardson, P.; Gagnon, K. J.; Teat, S. J.; Lorusso, G.; Evangelisti, M.; Tang, J.; Stamatatos, T. C. New Dioximes as Bridging Ligands in 3d/4f-Metal Cluster Chemistry: One-Dimensional Chains of Ferromagnetically Coupled $\{Cu_6Ln_2\}$ Clusters Bearing Acenaphthenequinone Dioxime and Exhibiting Magnetocaloric Properties. *Cryst. Growth Des.* **2017**, acs.cgd.7b00011 DOI: 10.1021/acs.cgd.7b00011.

(76) Voronkova, V. K.; Galeev, R. T.; Shova, S.; Novitchi, G.; Turta, C. I.; Caneschi, A.; Gatteschi, D.; Lipkowski, J.; Simonov, Y. A. Exchange Interaction and Spin Dynamics in Pentanuclear Clusters, Cu3Ln2(ClCH2COO)12(H2O)8 (Ln = Nd3+, Sm3+,

Pr3+). *Appl. Magn. Reson.* **2003**, *25*, 227–247 DOI: 10.1007/BF03166687.

(77) Pavlishchuk, A. V.; Kolotilov, S. V.; Fritsky, I. O.; Zeller, M.; Addison, A. W.; Hunter, A. D. Structural Trends in a Series of Isostructural Lanthanide–copper Metallacrown Sulfates (Ln III = Pr, Nd, Sm, Eu, Gd, Dy and Ho): Hexaaquapentakis[μ 3 -glycinehydroxamato(2–)] sulfatopentacopper(II)lanthanide(III) Heptaaquapentakis[μ 3 -glycinehydroxamato(2. *Acta Crystallogr. Sect. C Cryst. Struct. Commun.* **2011**, *67*, m255–m265 DOI: 10.1107/S0108270111021780.

(78) Mezei, G.; Kampf, J. W.; Pan, S.; Poeppelmeier, K. R.; Watkins, B.; Pecoraro, V. L. Metallacrown-Based Compartments: Selective Encapsulation of Three Isonicotinate Anions in Non-Centrosymmetric Solids. *Chem. Commun.* **2007**, 11, 1148–1150 DOI: 10.1039/b614024f.

(79) Chaudhari, A. K.; Joarder, B.; Rivière, E.; Rogez, G.; Ghosh, S. K. Nitrate-Bridged "pseudo-Double-Propeller"-Type lanthanide(III)-copper(II) Heterometallic Clusters: Syntheses, Structures, and Magnetic Properties. *Inorg. Chem.* **2012**, *51*, 9159–9161 DOI: 10.1021/ic3012876.

(80) Jankolovits, J.; Kampf, J. W.; Maldonado, S.; Pecoraro, V. L. Voltammetric Characterization of Redox-Inactive Guest Binding to Ln III[15-Metallacrown-5] Hosts Based on Competition with a Redox Probe. *Chem. - A Eur. J.* **2010**, *16*, 6786–6796 DOI: 10.1002/chem.200903015.

(81) Wu, J.; Zhao, L.; Zhang, L.; Li, X. L.; Guo, M.; Tang, J. Metallosupramolecular Coordination Complexes: The Design of Heterometallic 3d-4f Gridlike Structures. *Inorg. Chem.* **2016**, 55, 5514–5519 DOI: 10.1021/acs.inorgchem.6b00529.

(82) Zaleski, C. M.; Lim, C. S.; Cutland-Van Noord, A. D.; Kampf, J. W.; Pecoraro, V. L. Effects of the Central Lanthanide Ion Crystal Radius on the 15-MCCu II(N)pheHA-5 Structure. *Inorg. Chem.* **2011**, 50, 7707–7717 DOI: 10.1021/ic200740h.

(83) Li, L.; Zhang, Y.; Avdeev, M.; Lindoy, L. F.; Harman, D. G.; Zheng, R.; Cheng, Z.; Aldrich-Wright, J. R.; Li, F. Self-Assembly of a Unique 3d/4f Heterometallic Square Prismatic Box-like Coordination Cage. *Dalton Trans.* **2016**, *45*, 9407–9411 DOI: 10.1039/C6DT01651K.

(84) Andruh, M.; Ramade, I.; Codjovi, E.; Guillou, O.; Kahn, O.; Trombe, J. C. Crystal Structure and Magnetic Properties of [Ln2Cu4] Hexanuclear Clusters (Where Ln = Trivalent Lanthanide). Mechanism of the gadolinium(III)-copper(II) Magnetic Interaction. *J. Am. Chem. Soc.* **1993**, *115*, 1822–1829 DOI: 10.1021/ja00058a029.

(85) Feltham, H. L. C.; Brooker, S. Review of Purely 4f and Mixed-Metal Nd-4f Single-Molecule Magnets Containing Only One Lanthanide Ion. *Coord. Chem. Rev.* **2014**, *276*, 1–33 DOI: 10.1016/j.ccr.2014.05.011.

(86) Llunell, M.; Casanova, D.; Cirera, J.; Alemany, P.; Alvarez, S.; SHAPE: Program for the Stereochemical Analysis of Molecular Fragments by Means of Continuous Shape Measures and Assosciated Tools, Version 2.1, Barcelona. SHAPE: Program for the Stereochemical Analysis of Molecular Fragments by Means of Continuous Shape Measures and Assosciated Tools. Barcelona 2013.

(87) Andruh, M.; Ramade, I.; Codjovi, E.; Guillou, O.; Kahn, O.; Trombe, J. C. Crystal Structure and Magnetic Properties of [Ln2Cu4] Hexanuclear Clusters (Where Ln = Trivalent Lanthanide). Mechanism of the gadolinium(III)-copper(II) Magnetic Interaction. *J. Am. Chem. Soc.* **1993**, *115*, 1822–1829 DOI: 10.1021/ja00058a029.

(88) Ishida, T.; Watanabe, R.; Fujiwara, K.; Okazawa, A.; Kojima, N.; Tanaka, G.; Yoshii, S.; Nojiri, H. Exchange Coupling in TbCu and DyCu Single-Molecule Magnets and Related Lanthanide and Vanadium Analogs. *Dalton Trans.* **2012**, *41*, 13609–13619 DOI: 10.1039/c2dt31169k.

(89) Chandrasekhar, V.; Senapati, T.; Dey, A.; Das, S.; Kalisz, M.; Clérac, R. Cyclo- and Carbophosphazene-Supported Ligands for the Assembly of Heterometallic (Cu 2+/Ca 2+, Cu 2+/Dy 3+, Cu 2+/Tb 3+) Complexes: Synthesis, Structure, and Magnetism. *Inorg. Chem.* **2012**, *51*, 2031–2038 DOI: 0.1021/ic2014638.

(90) Elmali, A.; Elerman, Y. Magnetic Properties and Structure of a CuIIDyIII Heterodinuclear Schiff Base Complex. *J. Mol. Struct.* **2005**, *737*, 29–33 DOI: 10.1016/j.molstruc.2004.10.007.

(91) Costes, J.-P.; Dahan, F.; Dupuis, A.; Laurent, J.-P. Nature of the Magnetic Interaction in the (Cu^{2+}, Ln^{3+}) Pairs: An Empirical Approach Based on the Comparison Between Homologous (Cu^{2+}, Ln^{3+}) and ($Ni^{2+}{}_{LS}$, Ln^{3+}) Complexes. *Chem. - A Eur. J.* **1998**, *4*, 1616–1620 DOI; 10.1002/(SICI)1521-3765(19980904)4:9<1616::AID-CHEM1616>3.0.CO;2-A.

(92) Koner, R.; Lin, H.-H.; Wei, H.-H.; Mohanta, S. Syntheses, Structures, and Magnetic Properties of Diphenoxo-Bridged M(II)Ln(III) Complexes Derived from N,N'-ethylenebis(3-Ethoxysalicylaldiimine) (M = Cu or Ni; Ln = Ce-Yb): Observation of Surprisingly Strong Exchange Interactions. *Inorg. Chem.* **2005**, *44*, 3524–3536 DOI: 10.1021/ic048196h.

(93) Towatari, M.; Nishi, K.; Fujinami, T.; Matsumoto, N.; Sunatsuki, Y.; Kojima, M.; Mochida, N.; Ishida, T.; Re, N.; Mrozinski, J. Syntheses, Structures, and Magnetic Properties of Acetato- and Diphenolato-Bridged 3d–4f Binuclear Complexes [M(3-MeOsaltn)(MeOH) X (ac)Ln(hfac) 2] (M = Zn II , Cu II , Ni II , Co II ; Ln = La III , Gd III , Tb III , Dy III ; 3-MeOsaltn = N,N ′-Bis(3-Met. *Inorg. Chem.* **2013**, *52*, 6160–6178 DOI: 10.1021/ic400594u.

(94) Luis, F.; Bartolomé, J.; Fernández, J. F.; Tejada, J.; Hernández, J. M.; Zhang, X. X.; Ziolo, R. Thermally Activated and Field-Tuned Tunneling in Mn12Ac Studied by Ac Magnetic Susceptibility. *Phys. Rev. B* **1997**, *55*, 11448–11456 DOI: 10.1103/PhysRevB.55.11448.

(95) Bartolomé, J.; Filoti, G.; Kuncser, V.; Schinteie, G.; Mereacre, V.; Anson, C. E.; Powell, A. K.; Prodius, D.; Turta, C. Magnetostructural Correlations in the Tetranuclear Series of { Fe3 LnO2 } Butterfly Core Clusters: Magnetic and M??ssbauer Spectroscopic Study. *Phys. Rev. B - Condens. Matter Mater. Phys.* **2009**, *80*, 14430 DOI: 10.1103/PhysRevB.80.014430.

Stepwise investigation of the influences of steric groups versus counter ions to target Cu/Dy complexes

Irina A. Kühne, Kieran Griffiths, Amy-Jayne Hutchings, Oliver P. E. Townrow, Andreas Eichhöfer, Christopher E. Anson, George E. Kostakis, and Annie K. Powell

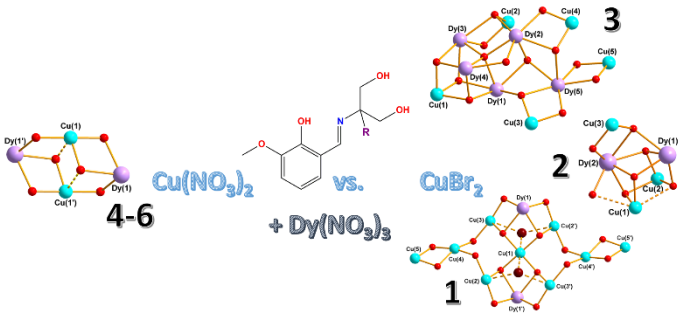

Based on an attempt to show the influence of a sterical group on a quite flexible ligand, we can show a family of structures which were formed by similar reaction conditions, where even small changes from a hydrogen atom over to a methyl to an ethyl group on the ligand has influence on the structure, depending on the used metal source.